Astronomy & Astrophysics manuscript no. astroph˙DUNES˙colddiscs
October 24, 2011

Letter to the Editor

Herschel discovery of a new class of cold, faint debris discs⋆

C. Eiroa[1], J. P. Marshall[1], A. Mora[2], A. V. Krivov[3], B. Montesinos[4], O. Absil[5], D. Ardila[6], M. Arévalo[4], J.-Ch. Augereau[7], A. Bayo[8], W. Danchi[9], C. del Burgo[10], S. Ertel[11], M. Fridlund[12], B.M. González-García[13], A. M. Heras[12], J. Lebreton[7], R. Liseau[14], J. Maldonado[1], G. Meeus[1], D. Montes[15], G.L. Pilbratt[12], A. Roberge[9], J. Sanz-Forcada[4], K. Stapelfeldt[16], P. Thébault[17], G. J. White[18,19], and S. Wolf[11]

(Affiliations can be found after the references)

Preprint online version: October 24, 2011

ABSTRACT

We present *Herschel* PACS 100 and 160 μm observations of the solar-type stars α Men, HD 88230 and HD 210277, which form part of the FGK stars sample of the Herschel Open Time Key Programme (OTKP) *DUNES* (*DU*st around *NE*arby *S*tars). Our observations show small infrared excesses at 160 μm for all three stars. HD 210277 also shows a small excess at 100 μm, while the 100 μm fluxes of α Men and HD 88230 agree with the stellar photospheric predictions. We attribute these infrared excesses to a new class of cold, faint debris discs. α Men and HD 88230 are spatially resolved in the PACS 160 μm images, while HD 210277 is point-like at that wavelength. The projected linear sizes of the extended emission lie in the range from $\sim$ 115 to $\leq$ 250 AU. The estimated black body temperatures from the 100 and 160 μm fluxes are $\lesssim$ 22 K, while the fractional luminosity of the cold dust is $L_{dust}/L_\star \sim 10^{-6}$, close to the luminosity of the Solar-System's Kuiper belt. These debris discs are the coldest and faintest discs discovered so far around mature stars and cannot easily be explained by invoking "classical" debris disc models.

Key words. - Stars: planetary systems: planetary discs -Stars: planetary systems: formation - Stars: individual: α Men (HIP 29271) - Stars: individual: HD 88230 (HIP 49908) - Stars: individual: HD 210277 (HIP 109378)

1. Introduction

Debris discs are tenuous structures associated with main sequence stars formed by second generation dust, which has resulted from the collisions of solid bodies continuously supplying the circumstellar environment with small dust particles. This formation sequence is inferred from the lifetime of the dust grains against destructive collisions, Poynting-Robertson drag and radiation pressure, which is much shorter than the ages of the host stars. These discs are visible in reflected light at optical wavelengths and in thermal radiation at mid-/far-IR and submillimeter wavelengths (Aumann et al., 1984; Backman & Paresce, 1993). General disc characteristics are grain black body temperatures of $\sim 50-100$ K, fractional luminosities $f > L_{dust}/L_\star \sim 10^{-5}$, and radii from less than 10 AU to several times 100 (e.g. Absil et al. 2006, Su et al. 2005, Trilling et al. 2008). Debris discs are considered analogues of the Solar System asteroid and Kuiper belts, although their luminosities are usually more than 100 times the Kuiper belt level of $L_{dust}/L_{Sun} \sim 10^{-7} - 10^{-6}$ (Stern 1996, Vitense et al. 2010). The sensitivity of the 3.5 m *Herschel* far-infrared space telescope (Pilbratt et al. 2010) with its instrument PACS (Poglitsch et al. 2010) offers the possibility of characterising colder ($\sim$ 30 K) and fainter ($L_{dust}/L_\star$ few times 10^{-7}) debris discs with spatial resolution $\sim$ 60 AU (FWHM) at 10 pc, i.e., true extra-solar Kuiper belts.

DUNES is a *Herschel* OTKP designed to detect and characterise extra-solar analogues to the Kuiper belt around main sequence FGK nearby stars (Eiroa et al. 2010). In this letter we present the results for three stars from the DUNES sample: α Men, HD 88230, and HD 210277 as clear examples of the advantages offered by *Herschel* observations: they trace a new class of cold, $T \lesssim 22$ K, spatially resolved debris discs with very low fractional luminosities. These discs have remained unobserved by previous far-IR and submillimeter studies. Table 1 gives some properties of the stars. Ages are based on the log R'_{HK} activity index and have an uncertainty of 60% (Mamajek & Hillenbrand 2008). HD 210277 hosts a Jupiter-like planet (Marcy et al. 1999). This star and α Men have faint stellar companions, but neither the measurements nor the photospheric predictions are affected by them. Eiroa et al. *in prep* will present a full discussion of the stars and the general results of the DUNES survey.

Table 1. Stellar properties.

Star	α Men	HD 88230	HD 210277
Sp. Type	G5V-G7V	K6V-M0V	G0V, G7V-G9V
Distance (pc)	10.2	4.9	21.6
$L_*(L_\odot)$	0.85	0.15	1.10
T_{eff}(K)	5590	3850	5540
Age (Gyrs)	5.5	6.6	6.9

2. Observations and data reduction

α Men, HD 88230 and HD 210277 were observed with PACS 100/160 μm in scan map mode. For each star, two scans at position angles 70° and 110° were carried out, each scan consisting of 10 legs with separation of 4″, length of 3′ and medium speed of 20″/s. Table 2 gives the scan identification numbers (Obs. ID) and the total duration of the observations (OT). α Men was observed twice in order to increase the S/N ratio. Data

⋆ Herschel is an ESA space observatory with science instruments provided by European-led Principal Investigator consortia and with important participation from NASA.

Table 2. Log of the PACS 100 μm and 160 μm observations.

Star	HIP	Obs. ID	OT (sec)
α Men	29271	1342203297/8	1116
α Men		1342216043/4	2244
HD 88230	49908	1342210610/1	4500
HD 210277	109378	1342211126/7	4500

reduction was made using the Herschel Interactive Processing Environment (HIPE) version 7.2. The individual scans were mosaiced to produce the final image at each band. To check the consistency of the reduction and analysis (particularly regarding the effect of correlated noise), mosaics were produced at both the native 3.″2 for 100 μm (green) and 6.″4 for 160 μm (red), as well as super-sampled pixel scales 1.0″ (green) and 2.0″ (red), the latter being the default pixel size in HIPE for this type of data. The images with the native pixel size scales avoid, at least partly, the correlated noise in the PACS images[1] (see also Fruchter & Hook, 2002). A high-pass filter was used to remove large scale background emission from the images, with filter widths of 15″ and 25″ in the green and red channels. To prevent the removal of any extended structure near the stars, regions where the sky brightness exceeded a threshold value in the image defined by the standard deviation of all the positive pixels ($S > 10^{-6} Jy/pixel$) were masked from that process. Absolute flux calibration uncertainties are ∼3% and ∼5% for the green and red bands (see technical note below).

3. Results

Table 3 gives the J2000.0 optical equatorial coordinates of the stars as well as their 100 μm peak positions corrected for the proper motions of the stars (van Leeuwen, 2007). Offsets between the optical and the PACS positions (column 4 of Table 3) are within ∼ 1.5σ the Herschel pointing accuracy of 2.″4 in this observing mode (Sánchez-Portal, private communication).

Fig. 1 shows the 100 and 160 μm images and isocontour plots of the stars. α Men and HD 88230 are point-like at 100 μm, FWHM ∼ 6.″3 × 6.″5, while both stars are resolved at 160 μm, with angular sizes/position angles ∼ 18″/52° and ∼ 23.″5/45°, respectively. The extended emission appears clearly asymmetric in HD 88230, with the star located at the North-Eastern side. None of the objects are resolved in the direction orthogonal to the extended emission. HD 210277 is unresolved at both wavelengths.

PACS fluxes (Table 3) have been estimated using circular and rectangular aperture photometry, taking special care to choose the reference background region due to the presence of field objects. Specifically, measurements of HD 210277 take into account the presence of the bright object located at ∼16″ North-East from the star; in the case of this star we have, in addition, carried out PSF photometry using the DAOPHOT software package. The PSF photometry fluxes are $F(100)$ = 8.4±0.3 mJy and $F(160)$ = 14.3±0.4 mJy (errors are those of the PSF fits), which are consistent with the aperture photometry estimates. Errors have been estimated using a variety of methods, including circular and rectangular boxes at different positions in the nearby fields. Sky sizes for the errors estimates are equal to the area of the aperture used for the photometry for all three stars and both bands; in particular the sizes of the extended emission around α Men and HD 88230.

PACS fluxes have been compared to predicted stellar photospheric fluxes (Table 3) using Gaia/PHOENIX models (Brott & Hauschildt, 2005), with the stellar parameters as given in Eiroa et al. (in prep). Fig. 1 shows the spectral energy distributions (SEDs) of the stars, where PACS fluxes are plotted together with optical, near-IR, IRAS, AKARI, and *Spitzer*/MIPS and IRS data; in addition, the best χ-square photospheric fit is shown. To assess the presence of an excess at 100 and/or at 160 μm we require that the observed fluxes, $F_{\rm PACS}$, exceed by at least 3σ the predicted photospheric fluxes, F_* ($\chi_\lambda = (F_{\rm PACS} - F_*)/\sigma_\lambda$). No excesses are detected at 100 μm for α Men and HD 88230, while it is seen in HD 210277. All three stars do show 160 μm excesses. We also note that the SED slopes from 100 to 160 μm are α = - 0.5±0.7 (α Men), α = - 0.7±0.6 (HD 88230), and α = 0.8±0.8 (HD 210277), which clearly differ from the expected Rayleigh-Jeans behaviour (α = - 2.0) of a stellar photosphere in this wavelength regime.

3.1. Comments on the PACS images

All three fields show ∼ 2-3 red sources per square arcmin, which are likely to be background galaxies. In particular, there is a faint peak at ∼13″ towards the SW from HD 88230 and a bright one at ∼16″ towards the NE from HD 210277. We have consulted the NASA/IPAC extragalactic database to search for counterparts without finding any association. Although we cannot firmly exclude a coincidental alignment or contamination of a background source(s) in the line of sight of our stars, we think that it is unlikely for the *Herschel* sources presented here due to the close correlation between the optical and *Herschel* positions, and the photospheric predictions and the estimated *Herschel* 100 μm fluxes. In fact, following in a first approach the source counts by Berta et al. (2010), the average density of extragalactic sources with fluxes ∼ 6-7 mJy and ∼ 12 mJy - i.e., the measured excesses at 160 μm from α Men/HD 88230 and HD 210277, respectively (Table 3) - are 2/arcmin^2 and 0.7/arcmin^2. Thus, given the optical/160 μm offsets (Fig. 1) the a priori probability of an accidental alignment is very small, clearly smaller than 5%. We refer to a future paper (del Burgo et al., *in prep.*) for a detailed study on source contamination within the DUNES fields.

4. Analysis

The small PACS excesses above the photospheric fluxes are interpreted as due to cold debris discs around the stars. Black body dust temperatures, $T_{\rm dust}$, can be estimated from the 100 and 160 μm excess fluxes for HD 210277; in the case of α Men and HD 88230, an upper limit for $T_{\rm dust}$ can be calculated taking the 100 μm flux as 3σ statistical noise. $T_{\rm dust}$ for the three stars is $\lesssim$ 22 K (Table 4); the corresponding inner radii of discs with black body grains at this $T_{\rm dust}$, considering the luminosity of the stars, are also given in Table 4. Fig. 1 shows the excellent agreement between the combined SED of the stellar photospheric fits plus 22 K black bodies and the observed SEDs.

Deconvolution of the images can be used to estimate the true size of the resolved discs in α Men and HD 88230. Our method first removes the photospheric contributions from each image by subtracting a PSF with a peak scaled to the predicted photospheric flux level. The PSF model uses α Boötis images, rotated to match the roll angle of the telescope during the observations of the DUNES stars. After star subtraction, the images are deconvolved using both modified Wiener and Richardson-Lucy algorithms. The noise model takes into account that the main contributor is the telescope thermal emission. Both algorithms produce consistent results although with different noise patterns. Fig. 2 shows the 160 μm star-subtracted and the Wiener-deconvolved

[1] Technical Note PICC-ME-TN-037 in http://herschel.esac.esa.int

Table 3. Optical positions of the stars and of their PACS 100 identified counterparts. Observed PACS fluxes with 1σ statistical errors ($F_{\rm PACS}$), and predicted photospheric fluxes ($F_\star$). Flux units are mJy.

Star	Optical position (J2000.0)	PACS 100 μm position (J2000.0)	Offset	PACS 100 μm			PACS 160 μm		
			$''$	$F_{\rm PACS}$	$F_\star$	χ_{100}	$F_{\rm PACS}$	$F_\star$	χ_{160}
α Men	06 10 14.47 -74 45 11.0	06 10 14.53 -74 45 11.1	0.3	17.8±1.3	18.0	-0.2	14.4±2.0	7.0	3.7
HD 88230	10 11 22.14 +49 27 15.3	10 11 21.88 +49 27 17.2	3.2	22.5±0.9	25.7	-3.6	16.0±1.7	10.0	3.5
HD 210277	22 09 29.87 -07 32 55.2	22 09 30.08 -07 32 54.1	3.3	8.5±1.0	4.6	3.9	12.4±1.6	1.8	6.6

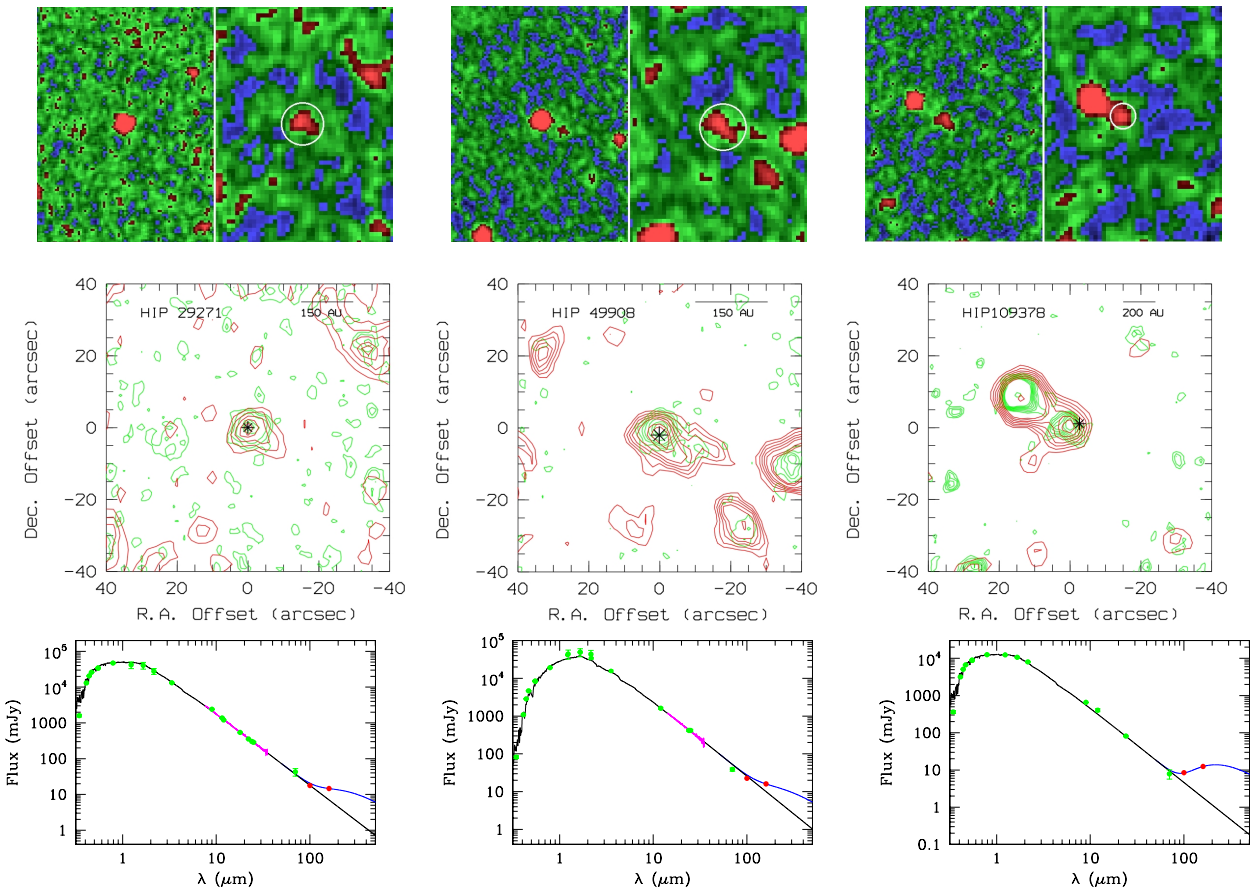

Fig. 1. PACS images, isocontours and SEDs of α Men/HIP 29271 (left), HD 88230/HIP 49908 (middle) and HD 210277/HIP 109378 (right). Images: 100 μm (left), 160 μm (right). North is up and East to the left. Isocontours: 100 μm contours are in green colour while the 160 μm ones are in red. α Men: 100 μm contours (10, 20, 40, 80 and 90 % of the flux peak); 160 μm contours (20,40,60,80, 90 % of the flux peak) HD 882308: 100 μm contours (10, 20,30,40,60, 80, 90 % of the flux peak); 160 μm contours (20, 30, 40, 50, 60, 80, 90 % of the flux peak) HD 210277: 100 μm contours ((30, 40, 50, 60, 70, 80, 90 % of the flux peak); 160 μm contours (50, 60, 70, 80, 90 % of the flux peak). The lowest contour in all cases is $\approx 3\sigma$. The optical position of the stars are indicated by the symbol "*" in the isocontour plots; a segment indicates the projected linear sizes at the distance of each star. SED plots: black line is the photospheric fit while the blue line is the photosphere plus a 22 K black body.

images of α Men and HD 88230; estimated sizes of the deconvolved sources are 16$''$ and 21$''$, respectively. Table 4 gives the linear sizes of the semi-major axes ($\sim 3\sigma$ contours) from both the original and deconvolved PACS 160 μm images. In the case of HD 210277, the value in Table 4 corresponds to an upper limit of 12$''$, i.e., approximately the 160 μm beam size. The comparison of both the directly observed and deconvolved semi-major axes to the estimated radii from $T_{\rm dust}$ clearly indicates that the observed discs (assuming as a first approach symmetric discs) are smaller than the expected sizes for black body discs.

Dust fractional luminosities, f (Table 4), can be obtained by taking the 160 μm fluxes and assuming the star temperatures given in Table 1 and $T_{\rm dust}$ = 22 K (Beichman et al., 2006). The estimated f values are of the order of 10^{-6}, close to the Kuiper belt level. Essentially similar f values are obtained taking the maximum wavelength corresponding to 22 K, i.e., 230 μm, and its expected flux extrapolating from the one measured at 160 μm.

5. Discussion

The debris discs in this work are a new class of discs characterised by an excess at 160 μm, little to no excess at 100 μm, and no excess emission at shorter wavelengths. These discs are the coldest and least luminous ones known to date; they are significantly colder and fainter than other observed DUNES discs

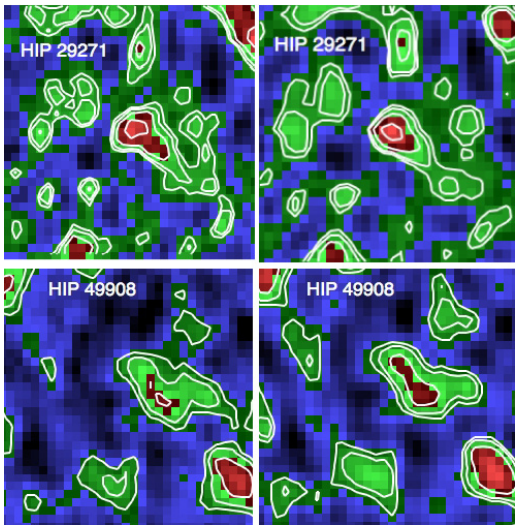

Fig. 2. 160 μm star-subtracted (left) and deconvolved (right) images. Up: α Men/HIP 29271. Contours: 10%, 20%,40%, 80% of the peak. Bottom: HD 88230/HIP 49908. Contours: 20%,40%, 80% of the peak. North is up and East to the left. Field size is $60'' \times 60''$.

Table 4. Black body dust temperatures from the far-IR excesses, $T_{\rm dust}$ and the corresponding estimated radii. Observed 3σ linear sizes (semi-major axes) of the extended emission at 160 μm in the original and deconvolved images. f is the dust fractional luminosity.

Star	$T_{\rm dust}$ (K)	Size Est. (AU)	Size Orig. (AU)	Size Deconv. (AU)	f
α Men	≤ 22	$\geq$147	92	81	9.7×10^{-7}
HD 88230	≤ 22	$\geq$62	56	51	1.6×10^{-6}
HD 210277	22	160	$\leq$130		5.4×10^{-6}

(e.g. Liseau et al. 2010, Marshall et al. 2011). Their interpretation poses significant challenges.

The shapes of the SEDs suggest that the dust is located in a ring with a larger inner void. We have seen that the observed disc radii are smaller than those implied from $T_{\rm dust}$ (Table 4). In other words, $T_{\rm dust}$ is smaller than the black body temperature, $T_{\rm bb} \approx$ 25-30 K, given the observed sizes and stellar luminosities. Thus, we need to reconcile these seemingly contradictory results. Since one would reasonably expect a broad grain size distribution, which would include small grains hotter than those indicated by the estimated $T_{\rm dust}$, the question is how to make the dust cold, while allowing a size distribution, but still keeping the disc radii within the observed ones.

The low temperatures of grains require them to be large and highly reflective. The required albedo can be derived from $T_{\rm dust}$ and $T_{\rm bb}$. Taking $T_{\rm dust}$ = 22 K as representative for the three observed discs, and $T_{\rm bb}$ = 25-30 K, the albedo would be $\gtrsim$50%. For comparison, surfaces of trans-Neptunian objects contain significant amounts of ice (Barucci et al. 2011) and many, especially large ones (e.g. Pluto, Eris), have albedos in excess of 50% (e.g. Vitense et al. 2010). Accordingly, Pluto has a surface brightness temperature $\sim$ 10 K below the black body value (Gurwell et al. 2010). It is natural to expect that dust released from the surfaces of such objects would have similar properties.

In addition, one has to explain why small grains in the cold discs are depleted. One possibility is to assume a very low dynamical excitation of dust-producing planetesimals, so that discs would be devoid of small particles (Thébault & Wu, 2008). The reason is that low collision velocities between large grains, unaffected by radiation pressure, create an imbalance between the rates at which small grains are produced (low) and destroyed (high). Low collision velocities are compatible with low orbital velocities at the large radii of the cold discs. Besides, since the surface density of the solids far from the central stars is also low, planetesimal accretion scenarios predict very long accretion timescales (Kenyon & Bromley, 2008). Thus, large planetesimals that would excite the discs may have failed to grow. In fact, low dynamical excitation has been inferred for other large debris discs, e.g. HD 207129 (Löhne et al 2011).

The tenet that the cold discs are probably in a low dynamical excitation state would be difficult to reconcile with the existence of large planets in the discs, since they would stir the discs too strongly. The emission around α Men and HD 88230 is asymmetric, which might be suggesting the presence of a giant planet as in Fomalhaut (Kalas et al.2008). The problem can be mitigated if the planets are in nearly-circular orbits or the planetesimals have low eccentricities, as suggested for Fomalhaut (Chiang et al. 2009). HD 210277 hosts a planet at 1.1 AU with e_p = 0.47; however, based on the formulae by Mustill & Wyatt (2009), a stirring front from such a planet should not be able to reach the $\sim$ 130 AU-sized disc on Gyr timescales.

Another point is the origin of the large inner voids in the cold discs. These could either be due to clearing by planets or may reflect the accretional and collisional history of primordial discs. In the latter case, the observed radii are those at which solids could reach "right" sizes, "right" degree of dynamical excitation, and/or were able to survive over the stellar age, to produce the observed emission. A detailed analysis of the nature of the cold discs is beyond the scope of this paper, and we defer to Krivov et al. (*in prep.*) where possible scenarios will be discussed in detail.

6. Conclusions

We have presented *Herschel* PACS observations of three stars of the OTKP DUNES sample. The observations reveal a new class of debris discs with fractional luminosities close to the Solar-System Kuiper's belt, but are colder and larger. These discs are a challenge to current models explaining debris discs around mature solar-type stars such as either the usual collisional-dominated disc scenario or low dynamical excitation discs.

References

Absil, O., di Folco, E., Mérand, A. et al. 2006, A&A 452, 237 2010 A&A 518, L17
Aumann H.H., Beichman, C.A., Gillet, F. C., et al. 1984 ApJ 278, L23
Backman, D.E., & Paresce, F. 1993, in Protostars and Planets III, ed. E.H. Levy & J.I. Lunine (Tucson: Univ. Arizona Press), 1253
Barucci, M. A., Alvarez-Candal, A., Merlin, F. et al 2011, Icarus 214, 297
Beichman, C.A., Bryden, G., Stapelfeldt, K.R., et al. 2006, ApJ 652, 1674
Berta, S., Magnelli, B. Lutz, D., et al. 2010 A&A 518, L30
Brott, I. & Hauschildt, P.H. 2005, ESA SP-576, C. Turon, K.S. O'Flaherty, M.A.C. Perryman (eds), p.565
Chiang, E., Kite, E., Kalas, P., Graham, J.R., Clampin, M. 2009, ApJ, 693, 734
Eiroa, C., Fedele, D., Maldonado, J., et al. 2010, A&A 518, L131
Fruchter, A. S.& Hook, R.R. 2002, PASP 114, 144
Gurwell, M. A., Butler, B. J., Moullet, A. 2010, BAAS 42, 1014
Kalas, P., et al. 2008, Science 322, 1345
Kenyon, S. J. & Bromley, B.C. 2008, ApJS, 179, 451
Liseau, R., Eiroa, C., Fedele, d., et al. 2010, A&A 518, L132
Löhne, T. et al. 2011, A&A, submitted

Mamajek,E. E., Hillenbrandt, L.A. 2008 ApJ 687, 1264
Marcy, G.W., Butler, R.P. Vogt S.S., Fischer, D., Liu, M.C. 1999 ApJ 520, 239
Mustill, A.J. & Wyatt, M.C. 2009, MNRAS, 399, 1403
Pilbratt, G., Riedinger, J. R., Passvogel, T., et al. 2010, A&A518, L1
Poglitsch, A., Waelkens, C., Geis, N., et al. 2010, A&A518, L2
Stern, S.A. 1996, A&A 310, 999
Su, K.Y.L., Rieke, G.H., Misselt, K.A., et al., 2005, ApJ 628, 487 653, 675
Thébault, P., Wu, Y 2008, A&A 481, 713
Trilling, D.F., Bryden, G., Beichman, C.A. et al. 2008, ApJ 674, 1086
van Leeuwen, F. 2007, A&A 474, 653
Vitense, Ch., Krivov, A. V., Löhne, T. 2010, A&A 520, 32

---

[1] Dpt. Física Teórica, Facultad de Ciencias, Universidad Autónoma de Madrid, Cantoblanco, 28049 Madrid, Spain e-mail: carlos.eiroa@uam.es
[2] ESA-ESAC Gaia SOC. P.O. Box 78, E28691 Villanueva de la Cañada, Madrid, Spain
[3] Astrophysikalisches Institut und Universitätssternwarte, Friedrich-Schiller-Universität, Schillergäßchen 2-3, 07745 Jena, Germany
[4] Dpt. de Astrofísica, Centro de Astrobiología (INTA-CSIC), ESAC Campus, P.O.Box 78, E-28691 Villanueva de la Cañada, Madrid, Spain
[5] Institut d'Astrophysique et de Géophysique, Université de Liege, 17 Allée du Six Août, B-4000 Sart Tilman, Belgium
[6] NASA Herschel Science Center, California Institute of Technology, 1200 E. California Blvd., Pasadena, CA 91125, USA
[7] Université Joseph Fourier/CNRS, Laboratoire d'Astrophysique de Grenoble, UMR 5571, Grenoble, France
[8] European Space Observatory, Alonso de Cordova 3107, Vitacura, Casilla 19001, Santiago 19, Chile
[9] NASA Goddard Space Flight Center, Exoplanets and Stellar Astrophysics, Code 667, Greenbelt, MD 20771.USA
[10] UNINOVA-CA3, Campus da Caparica, Quinta da Torre, Monte de Caparica, 2825-149 Caparica, Portugal
[11] Christian-Albrechts-Universität zu Kiel, Institut für Theoretische Physik und Astrophysik, Leibnizstr. 15, 24098 Kiel, Germany
[12] ESA Astrophysics & Fundamental Physics Missions Division, ESTEC/SRE-SA, Keplerlaan 1, NL-2201 AZ Noordwijk, The Netherlands
[13] INSA at ESAC, E-28691 Villanueva de la Cañada, Madrid, Spain
[14] Onsala Space Observatory, Chalmers University of Technology, Se-439 92 Onsala, Sweden
[15] Universidad Complutense de Madrid, Facultad de Ciencias Físicas, Dpt. Astrofísica, Av. Complutense s/n, 28040 Madrid, Spain
[16] Jet Propulsion Laboratory, California Institute of Technology, MS 183-900, 4800 Oak Grove Drive, Pasadena, CA 91109, USA
[17] LESIA, Observatoire de Paris, 92195 Meudon France
[18] Department of Physics and Astrophysics, Open University, Walton Hall, Milton Keynes MK7 6AA, UK
[19] Rutherford Appleton Laboratory, Chilton OX11 0QX, UK